Spin Reorientation and Structural Relaxation of Atomic Layers: Pushing the Limits of Accuracy

H. L. Meyerheim,[1,*] D. Sander,[1] R. Popescu,[1] J. Kirschner,[1] O. Robach,[2] and S. Ferrer[2]
[1]*Max-Planck-Institut für Mikrostrukturphysik, Weinberg 2, D-06120 Halle, Germany*
[2]*European Synchrotron Radiation Facility (ESRF), BP-220, F-38043 Grenoble, France*
(Received 14 January 2004; published 8 October 2004)

The correlation between an ad-layer-induced spin reorientation transition (SRT) and the ad-layer-induced structural relaxation is investigated by combined *in situ* surface x-ray diffraction and magneto-optical Kerr-effect experiments on Ni/Fe/Ni(111) layers on W(110). The Fe-induced SRT from in-plane to out-of-plane, and the SRT back to in-plane upon subsequent coverage by Ni, are each accompanied by a small lattice relaxation of at most 0.002 Å. Such a small strain variation excludes a magneto-elasticity driven SRT, and we suggest the interface anisotropy as a possible driving force.

DOI: 10.1103/PhysRevLett.93.156105 PACS numbers: 68.35.Ct, 61.10.–i, 75.30.Gw, 75.70.Ak

The magnetic anisotropy energy (MAE) is one of the key parameters of magnetic ultrathin films and nanostructures, and it is decisive for the exploration of the ultimate limits of the magnetic data storage density [1]. However, the MAE changes with reducing the size of the magnetic objects. The easy magnetization direction of atomic layers and of nanostructures deviates from the respective bulk values due to the ever increasing influence of lattice strain and surface effects with shrinking dimensions.

In general, the preferred orientations of the magnetization (M) are determined by a delicate balance between different competing contributions to the MAE. These are the shape anisotropy due to the magnetic dipole-dipole interaction ($\mu_0 M^2/2$) and the magnetocrystalline anisotropy (K) due to spin-orbit coupling. The former always favors in-plane magnetization of flat films, whereas winning of the latter can induce an easy out-of-plane magnetization direction.

Both experiment and theory show that the lattice-strain-induced tetragonal distortion of a cubic system is of paramount importance for the MAE [2]. This structural distortion leads to a magnetoelastic (ME) contribution to K, which determines the magnetic anisotropy in many cases. A prominent example is the magnetic anisotropy of Ni layers on Cu(001), where the tetragonal distortion (in-plane strain: $\epsilon_1 = +2.5\%$; out-of-plane strain: $\epsilon_3 = -3.2\%$) induces an out-of-plane easy magnetization direction in the coverage range 12–50 layers [3,4].

In this system as well as in many others an adsorbate-induced switching of the easy magnetization direction is observed [e.g., H/Ni/Cu(001) [4], O/Fe/Ag(001) [5], Ag/Fe/W(110) [6]]. Because of the lack of precise structural data the spin reorientation transition (SRT) is tentatively attributed to changes in the surface contribution to the MAE, while the influence of magnetoelastic contributions is neglected, although magnetoelasticity can be decisive even for small strains.

The correlation between lattice strain and magnetic aniostropy is given by the magnetoelastic coupling constants B_i, which couple the lattice strains ϵ_i to the MAE via terms $B\epsilon$ [2]. The large values of the B_i (Ni: $B_1 = 640\ \mu$eV/atom, $B_2 = 680\ \mu$eV/atom) [7] as compared to K (K_VBulk $= 0.4\ \mu$eV/atom), and the stray field energy ($\mu_0 M^2/2 = 11\ \mu$eV/atom), lead to a dominant contribution to the MAE even for moderate strains in the percent range. Thus, even subtle changes of the film structure have the potential to drive a SRT.

It is the goal of this Letter to elucidate whether the SRT of Ni(111) layers from in-plane magnetization to out-of-plane magnetization upon Fe-ad-layer coverage is accompanied by a respective structural change. The following condition must be fulfilled to overcome the shape anisotropy, $\Delta\varepsilon_3 > \mu_0 M^2/(2B_2)$. Inserting the values shows that the average vertical strain needs to contract by at least $\Delta d_{(111)}/d_{(111)} = \Delta\varepsilon_3 = 8 \times 10^{-3}$ corresponding to $\Delta d_{(111)} = 0.015$ Å. This is a small structural change, at the edge of current state-of-the-art surface structure analysis techniques.

At present there is no technique available allowing the analysis of lattice relaxation in the subpercent regime on an absolute basis. Here we followed a different path by measuring *in situ* the *relative changes* of the lattice spacings upon the ad-layer-induced SRT. Thus, a high sensitivity for minute structural changes in the subpercent range is achieved.

In this Letter we concentrate on the adsorbate-induced lattice relaxation and its potential impact on the magnetic anisotropy. Our combined *in situ* magneto-optical Kerr effect (MOKE) and surface x-ray diffraction (SXRD) experiments on several layer thin Ni(111) films on W(110) indicate that the change of the average film layer spacing $\Delta d_{(111)}$ is below 0.002 Å when the ad-layer-induced change of the easy magnetization axis from in-plane to out-of-plane occurs. Our results of unprecedented accuracy provide direct experimental evidence

that the ME contribution to the SRT is too low by one order of magnitude to drive the SRT. Instead, our experiments suggest that the ad-layer-induced change of the surface anisotropy is responsible for the SRT.

The experiments were carried out at the beam line ID3 of the European Synchrotron Radiation Facility (ESRF) in Grenoble using a six-circle ultrahigh-vacuum diffractometer operated in the z-axis mode at a wavelength of 0.73 Å [8]. MOKE experiments were performed *in situ* at the diffractometer chamber. The W(110) surface was cleaned by heating the sample ($12 \times 2 \times 0.1$ mm^3) several times at 1500 °C in 10^{-6} mbar oxygen partial pressure for 30 s. After a final flash at 2000 °C for 10 s the C contamination of the surface is lower than 1% of a monolayer (ML) as determined by Auger-electron spectroscopy. Ni deposition on the W(110) surface kept at room temperature was carried out by evaporation from a Ni rod heated by electron bombardment. The film thickness was measured by a quartz oscillator and by intensity oscillations of the diffracted intensity at the (001) antiphase condition (not shown). After deposition of the first layer the sample was annealed to 900 K for several minutes to promote the formation of a well ordered c-(1×7) structure [9] as a template for the subsequent deposition of Ni with a total thickness of 5, 8, and 10 atomic layers.

Ni films in this coverage range grow in a fcc(111)-like structure on the W(110) surface. The orientation between the Ni and the W lattices is described by the Nishiyama-Wassermann growth model [9,10]. Our growth procedure is optimized to obtain almost perfectly flat Ni(111) layers, which extend over approximately 100 nm wide W(110) terraces, as checked by scanning tunneling microscopy [11]. The stack of flat Ni layers gives rise to well defined side maxima in the SXRD scans (see below).

Figure 1 indicates the reflection positions in the symmetry independent part of the (hk) plane of the reciprocal space. All coordinates are referred to the substrate lattice,

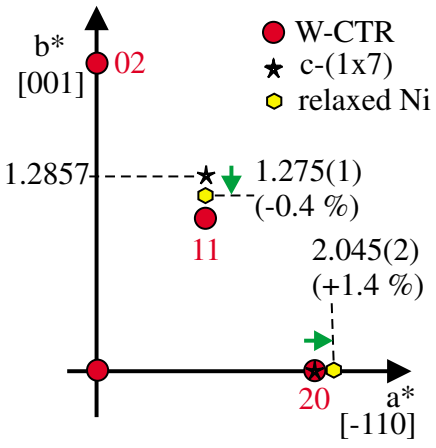

FIG. 1 (color online). (hk) plane of the reciprocal space. Arrows indicate the in-plane relaxation for an 8 layer Ni film. Values in parentheses indicate the strain with respect to bulk Ni(111).

where the large dark circles are the integer order crystal truncation rods (CTR) of the substrate. The reciprocal a^* and b^* axes are parallel to the $[\bar{1}10]$ and the [001] directions of the W(110) surface. The stars and the hexagons indicate reflections corresponding to the c-(1×7) and the fcc-like 8 layer Ni ad layer, respectively. Our previous studies have shown [9–11] that the c-(1×7) superstructure forms at the completion of the first Ni layer. Two characteristic reflections related to this structure are shown in the reciprocal lattice map at $(1, 1.2857)$ and $(2, 0)$, the latter coinciding with a W-CTR. At higher Ni coverage (≥ 3 atomic layers) a transition to a fcc-like Ni film takes place. This leads to a shift of the peak positions as indicated by the arrows in Fig. 1. The analysis of the peak positions (using the CTR reflections as reference) reveals that the 8 layer Ni film is still strained with respect to bulk Ni. We find an anisotropic in-plane strain with a compression of $\epsilon_1 = -0.004$ along W[001], and an expansion of $\epsilon_2 = +0.014$ along W$[\bar{1}10]$.

Before we discuss the vertical layer spacing in the Ni-layer stack in dependence of an ad-layer coverage, we present in Fig. 2 the magnetic hysteresis curves of 8 layers Ni on W(110), and after ad-layer coverage. Figure 2(a) shows magnetic hysteresis curves taken by MOKE measurements in the longitudinal geometry with the magnetic field applied in-plane along W[001] ≡ Ni$[\bar{1}10]$. The rect-

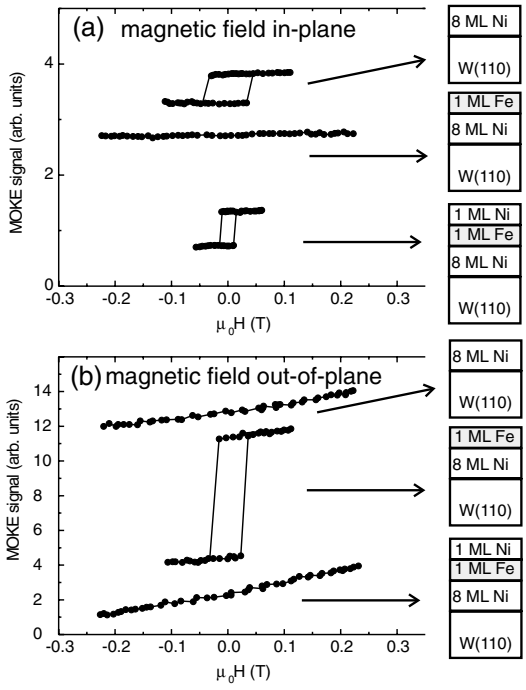

FIG. 2. Magnetic hysteresis curves from MOKE measurements at 300 K of 8 layer Ni on W(110), top curves, after coverage with one layer Fe, center curves, and after coverage with one Fe and one Ni layer, bottom curves. See sketch for layer sequence. (a) Magnetizing field in-plane along W[001] ≡ Ni$[\bar{1}10]$; (b) magnetizing field out-of-plane along W[110] ≡ Ni[111].

angular hysteresis of the top curve indicates an easy in-plane magnetization direction. Magnetization along the out-of-plane direction [see Fig. 2(b)] leads to a hysteresis-free magnetization curve, indicative of a hard axis magnetization direction. Upon coverage with Fe, the easy magnetization direction switches to out-of-plane (center curves in Fig. 2), and it reverts back to in-plane after capping the Fe layer with Ni (bottom curves in Fig. 2). Such an Fe-induced SRT has been previously discussed for thinner Ni films [12]. The SRT has been ascribed to the fcc phase of Fe, which forms on top of fcc-Ni(111) [12]. In the following we derive the magnitude of the ad-layer-induced structural relaxation along the film normal upon the ad-layer-induced SRT.

Figure 3 shows longitudinal SXRD scans along the (1 1.275) rod (see Fig. 1) of the fcc-Ni layer. The momentum transfer normal to the sample surface, $q_z = \ell \times c^*$, refers to $c^* = 1/4.476$ Å^{-1} as the reciprocal lattice unit (rlu), based on the W(110)-lattice metric. Longitudinal scans are appropriate to determine the relative change of the peak positions and peak widths along q_z. Moreover, for our experimental aims it is the method of choice, because it allows the collection of many data points along q_z within a short time. This is important to minimize sample contamination.

Scans were measured after deposition of 8 layers Ni (a), and subsequent deposition of one layer Fe (b), and another layer Ni (c). In total, three Bragg peaks are observed, where the first (α) and third (γ) can be indexed as the (101) and the (104) reflections of the fcc-like Ni structure satisfying the condition $-h + k + l = 3n$ ($n =$ integer), while the second (β) represents the reflection from the crystallographic twin related to the reversed layer stacking (ACB versus ABC). Between the main maxima also side maxima originating from the finite film thickness are visible, indicating a high degree of structural perfection. Between the SXRD scans, MOKE measurements were performed without any realignment of the sample orientation with respect to the primary beam. This procedure ensures the best possible sensitivity for the detection of small *relative* changes of the diffraction peak positions and profiles upon ad-layer coverage.

Both direct qualitative inspection of the peak positions and profiles and their quantitative analysis indicate that there are no differences between the experimental curves (a) to (c) within experimental resolution. The peaks were fitted by Gaussian functions. Highly accurate fits were obtained as indicated by the small residuals of the order of 2%–3% [13]. The first order reflection positions along q_z as derived from the fits of the peaks are shown in Fig. 4 for all samples investigated.

Experiments were performed for (i) 5 layers Ni plus one layer Fe (squares); (ii) 8 layers Ni plus one layer Fe, plus one layer Ni (circles); and (iii) 10 layers Ni plus one layer Fe, measured 3 times (diamonds), respectively. For all of these systems, the ad-layer-induced SRT as shown in Fig. 2 was observed. It should be emphasized that for each experiment a new preparation including high temperature flashing was carried out.

We first focus on the change of the peak position within each experiment. The shift of the *absolute* peak positions in experiment starting with 8 ML Ni as compared to the two other ones (initial Ni coverage 5 and 8 ML) is attributed to sample drift due to thermal treatment during preparation at the beginning of the whole experimental run. Adsorption of one ad layer does not lead to a shift of the peak positions larger than 5×10^{-4} to 1×10^{-3} rlu, which is only slightly larger than the reproducibility of the diffractometer settings in the order of 0.002° corresponding to 3×10^{-4} rlu. We therefore have a clear-cut experimental proof that the ad-layer-induced relaxation of the average vertical layer spacing is less than our

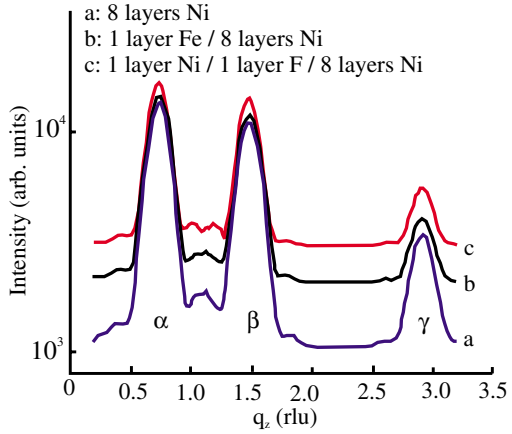

FIG. 3 (color online). Longitudinal scans along q_z of 8 atomic layers Ni on W(110) (a) and after subsequent deposition of one layer Fe (b) and one layer Ni (c). Peaks (α) and (γ) are related to the (101) and (104) reflection of the fcc-like structure, peak (β) is related to the crystallographic twin. The curves are shifted vertically for clarity.

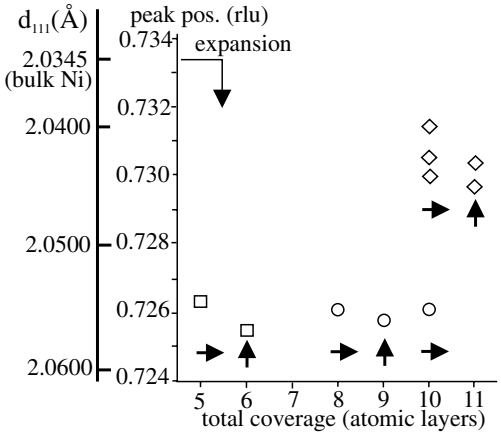

FIG. 4. First order peak (α) positions and interlayer distances derived from the diffraction curves. Squares, circles, and diamonds refer to different experiments starting with 5, 8, and 10 layers Ni. Arrows indicate the magnetization direction.

experimental accuracy of 10^{-3} rlu, corresponding to a lattice spacing relaxation of $\Delta d_{(111)} = 0.002$ Å. This is the most important result of our study.

In addition, the peak profiles were analyzed in order to detect structural inhomogeneities within the samples. First, there is no change in the peak shapes. All data could be fitted with equal accuracy using Gaussians, but the addition of one layer (Fe or Ni) to the film is reflected by a corresponding narrowing of the reflection full width at half maximum (FWHM) according to the relation $t[\text{Å}] = 0.886/\text{FWHM}\,[\text{Å}^{-1}]$ [14]. In this simple model the film is modeled by rectangular electron density of thickness t. The finite detector resolution of the order of 0.01 rlu along q_z was not considered in the data evaluation, since the FWHM's of the reflection curves are considerably larger (≈ 0.2 rlu) so that significant effects due to the finite resolution are not expected. A plot of the FWHM vs number of layers (not shown) yields a perfect linear relationship with a slope (thickness per layer), which agrees with the interlayer spacing ($\Delta d_{(111)} = 2.05$ Å), as derived from the absolute peak positions (see below). Thus we can exclude any kind of structural inhomogeneity since these would lead to reflection broadening.

The ME contribution to the MAE and its impact on the SRT is evaluated from the measured lattice strain. The in-plane strains are equal to $\epsilon_1 = -0.004$ and $\epsilon_2 = +0.014$ (see Fig. 1). We find an average peak position of all data presented in Fig. 4 of 0.728 ± 0.002 rlu. This corresponds to $d_{(111)} = 2.0495 \pm 0.006$ Å, and an out-of-plane strain $\epsilon_3 = +0.007$ with respect to bulk Ni(111) follows. Thus, we have evidence for a slight normal lattice expansion, which is in contrast to expectations from continuum elasticity, where a 0.3% contraction is predicted [2]. On first inspection this appears as a surprising result, but a similar behavior was observed for other systems as well [15]. These results indicate that continuum elasticity may lead to erroneous results for nonpseudomorphic layers.

On the basis of the experimentally derived stains and the relation $f_{\text{ME}} = \frac{1}{6}[B_1(\epsilon_1 - \epsilon_2) + B_2(5\epsilon_1 + \epsilon_2 - 6\epsilon_3)]$ for the ME contribution to the MAE [2], we find $f_{\text{ME}} = -7.4$ μeV, where the negative sign indicates that the ME coupling favors in-plane magnetization in agreement with experiment for the Ni(111) film.

On the other hand, the calculated lattice relaxation required to induce the SRT from in-plane to out-of plane ($\Delta d = 0.015$ Å) is roughly one order of magnitude larger than the experimentally determined one (0.002 Å). Therefore, we have direct experimental evidence that the ME contribution to the adsorption induced SRT is almost negligible and the SRT must be attributed to a change in the surface (interface) anisotropy K_S.

In summary, our combined *in situ* MOKE and SXRD analysis of the Ni/Fe/Ni/W(110) trilayer system indicates that subsequent Fe and Ni adsorption on a 5, 8, and 10 layer Ni films deposited on W(110) induces a SRT from in-plane to out-of-plane and back, respectively; the corresponding changes of the normal layer spacing are—if present—smaller than $\Delta d_{(111)} = 0.002$ Å. On the basis of this so far not achieved accuracy, the ME contribution to the total MAE could be evaluated. The experimentally derived lattice relaxation is about one order of magnitude too low to induce the SRT, which is therefore attributed to a change of the surface (interface) anisotropy K_S.

While this study is focused on Fe/Ni/W(110), we expect that our novel experimental approach to combine *in situ* MOKE with relative measurements of the interlayer relaxation is relevant for thin film magnetism in general. Since (adsorbate-induced) SRTs are a common phenomenon, but precise structural data are generally lacking, accurate structure determinations are clearly called for. The highly accurate structure data are important input for state-of-the-art calculations where there are different MAE contributions [16]. Our approach points to a solution of the long-standing problemof how to unravel the different anisotropy contributions that drive a SRT.

We (H. L. M. and D. S.) thank the ESRF for hospitality during our stay. The help of D. Ullmann during the experiments is also gratefully acknowledged.

*Electronic address: hmeyerhm@mpi-halle.mpg.de

[1] D. A. Thompson and J. S. Best, IBM J. Res. Dev. **44**, 311 (2000).
[2] D. Sander, Rep. Prog. Phys. **62**, 809 (1999).
[3] M. Farle, Rep. Prog. Phys. **61**, 755 (1998).
[4] R. Vollmer *et al.*, Phys. Rev. B **60**, 6277 (1999).
[5] S. D. Bader and J. L. Erskine, in *Ultrathin Magnetic Structures II*, edited by J. A. C. Bland and B. Heinrich (Springer, Berlin, 1994), Chap. 4.
[6] H. J. Elmers and U. Gradmann, Appl. Phys. A **51**, 255 (1990).
[7] M. B. Stearns, in *Magnetic Properties of 3d, 4d and 5d Elements, Alloys and Compounds*, Landolt-Börnstein Numerical Data and Functional Relationships in Science and Technology, Group III, Vol. 19a (Springer, Berlin, 1986).
[8] S. Ferrer and F. Comin, Rev. Sci. Instrum. **66**, 1674 (1995).
[9] H. L. Meyerheim *et al.*, Phys. Rev. B **67**, 155422 (2003).
[10] D. Sander, C. Schmidthals, A. Enders, and J. Kirschner, Phys. Rev. B **57**, 1406 (1998).
[11] C. Schmidthals, D. Sander, A. Enders, and J. Kirschner, Surf. Sci. **417**, 361 (1998).
[12] D. Sander *et al.*, J. Appl. Phys. **81**, 4702 (1997).
[13] The unweighted residual (R_u) is defined as $R_u = \sum |I_{\text{obs}} - I_{\text{calc}}| / \sum I_{\text{obs}}$, where I_{obs} and I_{calc} are the observed and calculated intensities, respectively, and the summation runs over all data points.
[14] John M. Cowley, *Diffraction Physics* (North-Holland Publishing, Amsterdam, 1981).
[15] R. Popescu *et al.*, Phys. Rev. B **68**, 155421 (2003).
[16] P. Weinberger and L. Szunyough, Comput. Mater. Sci. **17**, 414 (2000).